MITSUBISHI ELECTRIC RESEARCH LABORATORIES
https://www.merl.com

# PHYSICALLY-CONSTRAINED HYBRID MODELING FOR VAPOR COMPRESSION SYSTEMS

Dong, Yiyun; Qiao, Hongtao; Laughman, Christopher R.

TR2024-038 April 23, 2024

**Abstract**

Numerical simulations in the HVAC&R industries are crucial for optimizing advanced products, reducing costs, and meeting high-energy efficiency standards. Vapor compression system simulations can be broadly categorized into steady-state or transient. While steady-state evaluations determine system capacity and size, dynamic models offer a more realistic representation of system responses. Traditional dynamic models, based on the conservation laws, often lead to a complicated set of Differential Algebraic Equations (DAEs) that are challenging to solve numerically, especially for large-scale systems like variable refrigerant flow systems. Conversely, black-box models, derived directly from data, offer simplicity and accuracy within a specific operating range but lack flexibility when system architecture changes. In this paper, we propose a physically- constrained hybrid modeling framework for vapor compression systems. This approach adopts a modular based solution scheme so that arbitrary system configurations can be handled, i.e., components can be modeled with flexibility to use either data-driven or physics-based approach. In particular, we train and evaluate the Gated Recurrent Units (GRUs) component models for heat exchangers while use physics-based models for other components. A generic system solver is developed to evaluate the system configuration, formulate, and solve the resulting equations, fulfilling the conservation laws on the system level. A comprehensive comparison between this novel hybrid modeling framework and the traditional physics-based modeling approach is conducted, focusing on the aspects of system dynamics, prediction accuracy, and simulation speed.

*Thermal and Fluids Engineering Conference 2024*



Mitsubishi Electric Research Laboratories, Inc.
201 Broadway, Cambridge, Massachusetts 02139

# PHYSICALLY-CONSTRAINED HYBRID MODELING FOR VAPOR COMPRESSION SYSTEMS

**Yiyun Dong,[1] Hongtao Qiao,[2,*] & Christopher Laughman[2]**

[1]University of Washington, Seattle, WA, 98105, USA
[2]Mitsubishi Electric Research Laboratories, Cambridge, MA, 02139, USA

## ABSTRACT

Numerical simulations in the HVAC&R industries are crucial for optimizing advanced products, reducing costs, and meeting high-energy efficiency standards. Vapor compression system simulations can be broadly categorized into steady-state or transient. While steady-state evaluations determine system capacity and size, dynamic models offer a more realistic representation of system responses. Traditional dynamic models, based on the conservation laws, often lead to a complicated set of Differential Algebraic Equations (DAEs) that are challenging to solve numerically, especially for large-scale systems like variable refrigerant flow systems. Conversely, black-box models, derived directly from data, offer simplicity and accuracy within a specific operating range but lack flexibility when system architecture changes. In this paper, we propose a physically-constrained hybrid modeling framework for vapor compression systems. This approach adopts a modular based solution scheme so that arbitrary system configurations can be handled, i.e., components can be modeled with flexibility to use either data-driven or physics-based approach. In particular, we train and evaluate the Gated Recurrent Units (GRUs) component models for heat exchangers while use physics-based models for other components. A generic system solver is developed to evaluate the system configuration, formulate, and solve the resulting equations, fulfilling the conservation laws on the system level. A comprehensive comparison between this novel hybrid modeling framework and the traditional physics-based modeling approach is conducted, focusing on the aspects of system dynamics, prediction accuracy, and simulation speed.

**KEY WORDS:** vapor compression system, hybrid modeling, physics-based simulation, data-driven, recurrent neural network, dynamics

## NOMENCLATURE

***Symbols***

| | | | | | |
|---|---|---|---|---|---|
| $C_V$ | flow coefficient | ( - ) | $p$ | pressure | (Pa) |
| $f$ | frequency | (Hz) | $Q$ | thermal energy | (J) |
| $F_{res}$ | residual function | ( - ) | $RH$ | relative humidity | ( - ) |
| $h$ | specific enthalpy | $(\mathrm{J \cdot kg^{-1}})$ | $T$ | temperature | (K) |
| $\dot{m}$ | mass flow rate | $(\mathrm{kg \cdot s^{-1}})$ | $V$ | Volume | $(\mathrm{m^{-3}})$ |
| $M$ | mass | (kg) | | | |

***Greek Letters***

| | | | | | |
|---|---|---|---|---|---|
| $\alpha$ | mass flow rate model coefficient | ( - ) | $\rho$ | density | $(\mathrm{kg \cdot m^{-3}})$ |
| $\eta$ | efficiency | ( - ) | $\phi(\cdot)$ | function | |

*Corresponding Hongtao Qiao: qiao@merl.com

***Subscripts***

| | | | |
|---|---|---|---|
| *a* | air | *lat* | latent |
| *atm* | atmosphere | *out* | outlet |
| *com* | compressor | *ref* | refrigerant |
| *con* | condenser | *res* | residual |
| *dis* | discharge | *suc* | suction |
| *disp* | displacement | *t* | time |
| *eva* | evaporator | *tot* | total |
| *in* | inlet | *val* | valve |
| *isen* | isentropic | | |

# 1. INTRODUCTION

Contemporary architectural designs often feature buildings with high ceilings, operable windows, and extensive perimeter exposure. While improving aesthetic appeal and functionality, these designs significantly impact occupant comfort, indoor air quality, and energy consumption. To address the challenges and meet high-performance green buildings standards, a growing trend is to develop energy-efficient HVAC&R (Heating, Ventilation, Air Conditioning and Refrigeration) systems, which offers separate controls for temperature, ventilation, and dehumidification.

Optimizing the HVAC&R systems requires an understanding of building thermal properties and climatic variations. Due to the inherent complexities of HVAC&R systems, mathematical modeling and simulation become indispensable tools in design, eliminating the need for expensive and slow experimental setups. The vapor compression cycle-based HVAC&R systems, prevalent in contemporary commercial buildings, exhibit dynamical behaviors due to interaction physics across various time and length scales. Governed by conservation laws of physics, including mass, energy, and momentum [1], the mathematical models for these systems consist of numerous differential algebraic equations (DAEs), inherently nonlinear and stiff, posing challenges in finding the solution. Additionally, detailed fluid dynamics and heat transfer analysis, essential for physical modeling, are computationally intensive, unsuitable for real-time operations and control. As a result, achieving a balance between accuracy and computational efficiency becomes crucial for HVAC&R system models.

In contrast, black-box models, built directly from data without explicit knowledge of the underlying mechanisms, possess the advantage of simplicity and quantitative accuracy within the data ranges. Data-driven modeling techniques, especially artificial neural networks, have found applications in the evaluation and analysis of vapor compression systems [2–5] and the performance mapping of individual HVAC&R components [6–9]. However, existing literature of data-driven approaches for HVAC&R systems largely focuses on steady-state behavior or equilibrium, leading to insufficient representation of the intricate nonlinear dynamics between different HVAC&R components and the underlying transient states.

The drawback becomes more obvious when the data-driven approaches are applied directly at the system level. The data-driven models built from system data could not account for inner dynamics between different HVAC&R components. Moreover, these models demand extensive inputs and training data, especially for large-scale HVAC&R systems with complex heat exchanger (HEX) networks. Even slight changes in system architecture can render the data-driven model obsolete, requiring a time-consuming re-training with increased model dimensions. Given these challenges, a necessity emerges for a modeling approach that captures the nonlinear dynamic behavior and handles varying system configurations without requiring additional re-training. Therefore, our paper attempts to address this gap by proposing a hybrid modeling approach that leverages the advantages of both physics-based and data-driven modeling.

Our proposed hybrid modeling approach offers a novel solution, which:

- Adopts a Modular-Based Scheme: This provides flexibility in component modeling, allowing for choosing between data-driven or physics-based methods as needed. In this paper, we train autoregressive GRU models to capture the dynamics of HEXs, while using physics-based models to represent other components.
- Ensures System-Level Conservation Laws: A generic system solver guarantees that conservation laws are fulfilled, ensuring the reliability of the model.
- Improves Adaptability: The modular nature of the approach allows capabilities for handling arbitrary system configurations, addressing the limitations of traditional data-driven models.

Integrating the strengths of physics-based and data-driven modeling, our approach aims to inspire potential applications in the design and analysis of HVAC&R systems. Subsequent sections delve into component model and system solvers (Section 2), simulation results (Section 3), and conclusions (Section 4).

## 2. MODEL DEVELOPMENT

Our proposed method integrates physics-based models with data-driven techniques for vapor compression system simulations. This section starts with foundational physics-based models used for the compressor and expansion valve. Then we introduce data-driven approaches using Gated Recurrent Units (GRUs) for dynamic modeling of HEXs. Combining the component models, an iterative system solver is developed for our hybrid modeling framework. This section aims to elucidate the modeling choice of each component and the setup of hybrid modeling framework.

### 2.1 Physics-Based Compressor Modeling

In this work, the compressor is modeled by physical laws. Here we consider a variable-speed high-side rotary compressor, where the motor is cooled by compressed high-pressure discharge refrigerant [10].

The mass flow rate delivered by the compressor takes the following form

$$\dot{m}_{com} = \eta_V f \rho_{suc} V_{disp} \tag{1}$$

where $\eta_V$ is the volumetric efficiency of the compressor model. Here the refrigerant density $\rho_{suc}$ is computed from the suction pressure $p_{suc}$ and enthalpy $h_{suc}$.

The actual discharge enthalpy $h_{dis}$ is derived from the idealized performance of the compressor,

$$h_{dis} = h_{suc} + (h_{(dis,isen)} - h_{suc})/\eta_{isen} \tag{2}$$

where $\eta_{isen}$ represents the isentropic efficiency

$$\eta_{isen} = (h_{(dis,isen)} - h_{suc})/(h_{dis} - h_{suc}) \tag{3}$$

and $h_{(dis,isen)}$ denotes the ideal discharge enthalpy after isentropic expansion, determined by $p_{suc}, h_{suc}, p_{dis}$.

### 2.2 Physics-Based Expansion Valve Modeling

The expansion valve is also modeled physically. In our system, we consider a linear electronic expansion valve [10]. It can be described using a standard orifice-type relationship between the mass flow rate $\dot{m}_{val}$ and pressure drop $\Delta p$ across the valve,

$$\dot{m}_{val} = C_V \sqrt{\rho_{in} \Delta p} \tag{4}$$

where $C_V$ is the flow coefficient determined using experimental data and the pressure drop $\Delta p = p_{con} - p_{eva}$.

### 2.3 GRU-Based Data-Driven Modeling For HEXs

Problem formulation. The vapor compression cycle in this work contains both the condensing and evaporating HEXs. As the refrigerant flows through the HEXs, heat is transferred between HEXs and air, while the matter and momentum are exchanged between HEXs and other devices. The behavior of HEXs over time can then be considered as a function of matter, momentum, and energy exchanged through the interface between HEXs and the environment, such as air or refrigerant pipes. On the system-level, HEX components can be viewed as black-box functions without solving the internal dynamics. Considering the time discretization, the behavior of HEXs can be modeled as

$$y_t = \phi(u_0; x_t, x_{t-1}, \ldots, x_0) \equiv \phi(u_0, x_{0:t}) \tag{5}$$

However, tracking $x$ values over the entire period is both time and storage-intensive. Given that HEXs are highly dynamical and that their response at any given time step primarily depends on recent variations, the observable outputs $y$ at time $t$ can then be approximated using a history of $N$ previous time steps as

$$y_t = \phi'(x_{t-N:t}, y_{t-N:t-1}) \tag{6}$$

Here, $N$ denotes the number of past time steps considered to influence the current state. This approximation allows us to frame the problem for a data-driven autoregressive model, utilizing recent input-output data for predictions.

For the above formulations, the terms are defined as

- $y_t$: the observable outputs of the system at time $t$
- $x_{t_0:t}$: the time-varying boundary conditions (BCs) and the actuated state inputs through the period $[t_0, t]$
- $u_0$: the initial internal state of the system at $t = 0$.

*Parametrization.* To effectively capture the dynamics of HEXs, the input $x$ and output $y$ are defined as follows

$$\begin{aligned} x &= [\ \underbrace{T_{a,in} \quad RH_{a,in} \quad \dot{m}_{a,in} \quad p_{atm}}_{\text{air-side BCs}} \quad \underbrace{\dot{m}_{ref,in} \quad h_{ref,in} \quad h_{ref,out} \quad p_{ref,out}}_{\text{refrigerant-side BCs}} \quad M_{ref,tot}\ ] \\ y &= [\ p_1 \quad p_N \quad h_1 \quad h_N \quad Q_{tot} \quad Q_{lat} \quad \Delta\dot{m}_{ref}\ ] \end{aligned} \tag{7}$$

Here $M_{ref,tot}$ represents the total refrigerant mass inside the HEX tube, and $\Delta\dot{m}_{ref} = \dot{m}_{ref,out} - \dot{m}_{ref,in}$ represents the change-in mass flow rate of refrigerant through the HEX. Subscripts $\cdot_1$ and $\cdot_N$ respectively denotes a quantity at the first unit and last unit of the HEX tube.

For simplicity, we adopt the notation

$$x = [x_{air} \quad x_{ref}] \tag{8}$$

with the definitions

$$x_{air} \equiv [T_{a,in} \quad RH_{a,in} \quad \dot{m}_{a,in} \quad p_{atm}]\ ,\ x_{ref} \equiv [\dot{m}_{ref,in} \quad h_{ref,in} \quad h_{ref,out} \quad p_{ref,out} \quad M_{ref,tot}] \tag{9}$$

*GRU architecture.* Gated Recurrent Units (GRUs) serve as an effective architecture for approximating the underlying relationship $\phi'$ between inputs $x$ and outputs $y$ [11]. Building upon earlier parametrization and problem formulation, we model HEX dynamics using GRU architecture as inspired by Bhattacharya's previous work [12].

A GRU cell embodies three primary gate vectors: the reset gate $r_t$, the update gate $z_t$, and the new gate $n_t$. These gates contribute to updating the hidden state $h_t$ as follows

$$\begin{aligned} r_t &= \sigma(W_{ir}s_t + b_{ir} + W_{hr}h_{t-1} + b_{hr}) \\ z_t &= \sigma(W_{iz}s_t + b_{iz} + W_{hz}h_{t-1} + b_{hz}) \\ n_t &= \tanh(W_{in}s_t + b_{in} + r_t * (W_{hn}h_{t-1} + b_{hn})) \\ h_t &= (1 - z_t) * n_t + z_t * h_{t-1} \end{aligned} \tag{10}$$

Here $W$ denotes neural weights, $\sigma$ is the sigmoid function, and $*$ stands for the Hadamard product.

Fig. 1 provides a comprehensive overview of the GRU-based neural network structure. It involves 2 GRU layers, each with a pre-defined context length $N$ and prediction length $N'$, followed by a fully connected layer. To initialize a $N'$-step prediction starting at $T$, both input features $x$ and outputs $y$ of past time series are passed to the network. At each time step $t$ of the prediction phase, the hidden state $h_t$ is produced by the GRU layers from the network input $s_t$ and the previous hidden state $h_{t-1}$. Then the predicted output $\tilde{y}_t$, obtained from the transformation of $h_t$ through a fully connected layer, is subsequently concatenated with $x_{t+1}$ as next network input $s_{t+1}$. This procedure is repeated until the final prediction length is reached.

Each sample in the dataset has a time length of $N + N'$ with size $N$ of context and size $N'$ for prediction. During training, the mean-squared error between predicted outputs and ground truths are computed from all

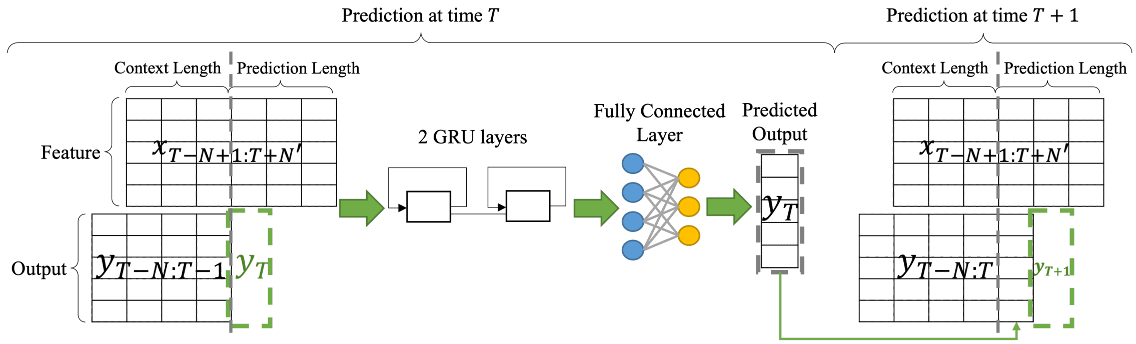


**Fig. 1** An illustration on the GRU architecture and the procedure of multi-step prediction.

samples as the total training loss

$$\text{total training loss} = \sum_{sample} \sum_{t=T}^{T+N'-1} \|y_t - \tilde{y}_t\|^2 \tag{11}$$

For multi-step inferences, a sliding window selects time series data input for each prediction iteration, with the GRU-based model forecasting the subsequent time step. This continues until the entire series prediction ends.

Overall, the adopted GRU architecture provides flexible context and prediction lengths, which can be adjusted across training and inference stages. The usage of student forcing mechanism ensures multi-step prediction accuracy. These features indicate the potential of GRU-based models for accurate HEX component dynamics simulation at the system level.

### 2.4 Hybrid Modeling Framework For System Integration

A vapor compression cycle operates on the principle of transferring heat from a low-temperature region to a high-temperature region using a refrigerant. This system consists of four basic components: the compressor, condenser, expansion valve, and evaporator, as depicted in Fig. 2(a).

In this study, we adopt a hybrid modeling framework using a modular-based scheme that combines data-driven techniques with traditional physics-based approaches, to leverage the strengths of both methodologies. Our approach, as discussed in the introduction, is potentially powerful because it provides flexibility in model selection for individual components and overall system configuration while ensuring system-level consistency. Specifically, the HEX components (condenser and evaporator) are modeled using GRU-based models, whereas the compressor and expansion valve are modeled using physical laws. At the system level, first principles are maintained by imposing conservation laws at the junctions between components. Dynamic mathematical relationships are established accordingly to handle arbitrary system configurations. An iterative system solver updates the thermodynamic states of each component, while preserving the conservation of mass, energy, and momentum throughout the system.

The detailed algorithm is shown in Fig. 2(b). Beginning at time $t_0$, all components are initialized with specified physical coefficients. At each time step $t$, the GRU models for the condenser and evaporator are activated with their respective inputs $x_t$ and contexts $x_{t-N:t-1}, y_{t-N:t-1}$, generating one-step inference. Based on the GRU outputs $y_{con,t}, y_{eva,t}$, the conservation laws of momentum and energy at the junctions update $p_{dis}, p_{eva}$ and $h_{suc}, h_{con}$, thereby providing inputs for the compressor and valve. The physics-based models for the compressor and valve, together with the mass conservation laws, then contribute to determining the refrigerant parameters for the subsequent GRU inputs at time $t+1$,

$$\begin{aligned} x_{con,ref,t+1} &= [\dot{m}_{com} \quad h_{dis} \quad h_{con,out} \quad p_{con} \quad M_{con,tot,t+1}] \\ x_{eva,ref,t+1} &= [\dot{m}_{val} \quad h_{eva} \quad h_{eva,out} \quad p_{suc} \quad M_{eva,tot,t+1}] \end{aligned} \tag{12}$$

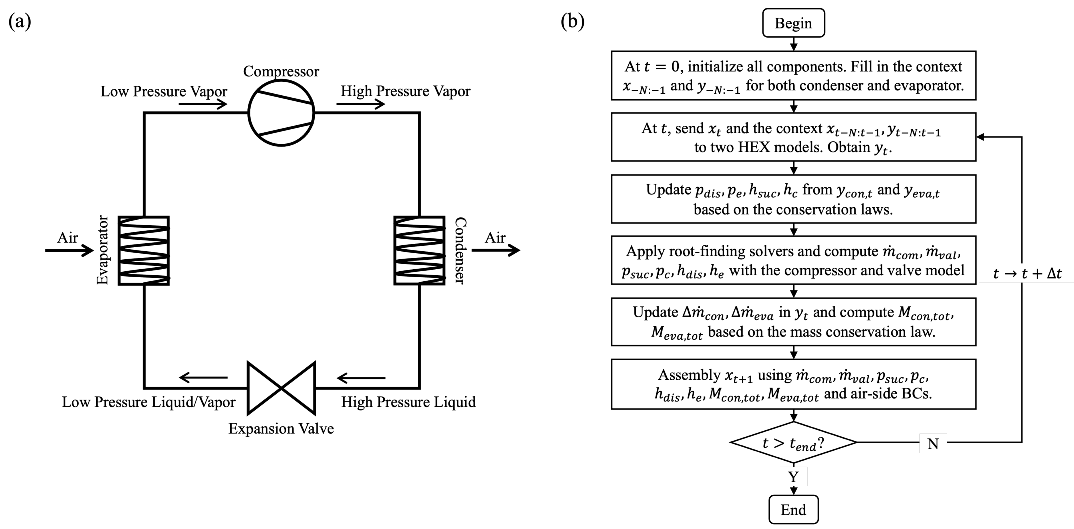


**Fig. 2** Hybrid modeling framework. (a) An example of the vapor compression system. (b) Flowchart illustrating the update mechanism of the hybrid modeling algorithm

Here $\dot{m}_{com}, \dot{m}_{val}, p_{suc}, p_{con}$ and $h_{dis}, h_{eva}$ are solved using root-finding algorithms, while $M_{tot,con}, M_{tot,eva}$ and the context for GRU models are both updated based on mass consistency, as detailed in the following paragraphs. With air-side BCs provided concurrently, this process is then repeated until the system reaches a steady state.

*Root-finding solver.* In order to determine outputs $\dot{m}_{com}, p_{suc}, h_{dis}$ from the compressor and $\dot{m}_{val}, p_{con}, h_{eva}$ from the valve, the root-finding algorithm using Newton's method is applied to solve the residual equations based upon the conservation of mass flows through junctions.

$$\begin{aligned} \text{(Compressor)} \quad F_{res}(p_{suc}) &= \dot{m}_{ref,out,eva}(p_{suc},\, p_{N,eva}) - \dot{m}_{com}(p_{suc},\, h_{suc}) \\ \text{(Valve)} \quad F_{res}(p_{con}) &= \dot{m}_{ref,out,con}(p_{con},\, p_{N,con}) - \dot{m}_{val}(p_c,\, p_e,\, h_c) \end{aligned} \tag{13}$$

Here $\dot{m}_{com}$ and $\dot{m}_{val}$ are computed using physics-based models of the compressor and valve (as described in Section 2.1 and 2.2). $\dot{m}_{out}$ denotes the outlet mass flow rate from the HEX component (evaporator or condenser), which is calculated using the following equation,

$$\dot{m}_{ref,out}(p_{out}, p_N) = \dot{m}_{0,out}(\frac{\Delta p}{\Delta p_0})^{\alpha}, \Delta p = p_N - p_{out} \tag{14}$$

Here $m_{0,out}$ and $p_0$ are respectively reference values for the mass flow rate and pressure drop at the end unit of the HEX tube, and $\alpha$ is a unitless factor selected as the best fit of the equation.

*Mass consistency.* To further maintain mass consistency through the system, $\dot{m}_{com}$ and $\dot{m}_{val}$ solved from the root-finding solver are used to update the change-in mass flow rates $\Delta m$ in the context of GRU models, as well as to compute the total masses $M_{tot}$ for the next input using the first order finite difference. Specifically,

$$\begin{aligned} \Delta\dot{m}_{con,t} &= \dot{m}_{com} - \dot{m}_{val} \\ \Delta\dot{m}_{eva,t} &= \dot{m}_{val} - \dot{m}_{com} \\ M_{con,tot,t+1} &= M_{con,tot,t} + \Delta\dot{m}_{con,t} \cdot \Delta t \\ M_{eva,tot,t+1} &= M_{eva,tot,t} + \Delta\dot{m}_{eva,t} \cdot \Delta t \end{aligned} \tag{15}$$

In summary, our hybrid modeling framework combines GRU-based models with traditional physics-based models for vapor compression systems, which benefits from the improvements in the predictive power, the consistency with conservation laws and system flexibility. By employing an iterative system solver and a root-finding approach, the framework maintains mass, energy, and momentum conservation across system components and junctions, inspiring accurate and efficient vapor compression system simulations.

# 3. MODELING RESULTS AND DISCUSSION

## 3.1 GRU Model For HEXs

Experiment setup. To data-driven models for HEX components, GRU architecture are adopted due to their auto-regressive nature in modeling time series, exhibiting potentials in understanding the dynamic behavior of HEXs. Separate GRU models were trained for the condenser and evaporator, utilizing datasets simulated with a library of thermofluid component models in Modelica, processed by the Dymola 2020x compiler. The refrigerant selected for this study was R134A, based on its common usage.

The condenser and evaporator datasets consist of 16000 and 8000 data points, respectively, with each data point spanning 100s and sampling with step size 1s. To mimic the dynamic behavior of the refrigerant within the HEXs, three refrigerant-side BCs — $\dot{m}_{ref,in}$, $h_{ref,in}$ and $p_{ref,out}$ — were varied by random ramp changes at arbitrary intervals. Simultaneously, $M_{ref,tot}$ fluctuated accordingly with these BCs, while $h_{ref,out}$ was maintained at a constant $330\mathrm{kJ/kg}$, under the assumption of no reverse flow. The air-side BCs were kept constant, simulating a stable external environment, as detailed below:

$$\begin{aligned} &\text{(Condenser)} \quad T_{a,in} = 35.0°\mathrm{C},\ RH_{a,in} = 0.8,\ \dot{m}_{a,in} = 0.8,\ p_{atm} = 1.0133 * 10^5\mathrm{Pa}, \\ &\text{(Evaporator)} \quad T_{a,in} = 24.4°\mathrm{C},\ RH_{a,in} = 0.8,\ \dot{m}_{a,in} = 0.8,\ p_{atm} = 1.0133 * 10^5\mathrm{Pa} \end{aligned} \tag{16}$$

Our GRU models configured with a context length of $N = 2$ or $N = 20$ and a prediction size of $N' = 2$ were trained with a 9:1 train-to-validation split and normalized variable ranges. Each GRU layer consists of 128 latent features, in order to fully capture complex dynamics within the hidden space. The Adam optimizer is deployed to optimize training employed the Adam optimizer, initialized with a learning rate of 5e-4, which decreased tenfold upon observing no metric improvement over three epochs.

Results and discussion. The performance of GRU models, illustrate in Fig. 3, proves their ability to predict system behavior accurately, where $\dot{m}_{ref,out}$ is plotted instead of $\Delta\dot{m}_{ref}$ for better comparison with the inlet quantity $\dot{m}_{ref,in}$. In particular, the models exhibit relative errors within 1% during transient states and a remarkable 0.1% during steady states, revealing the accuracy of the GRU models in multi-step inference.

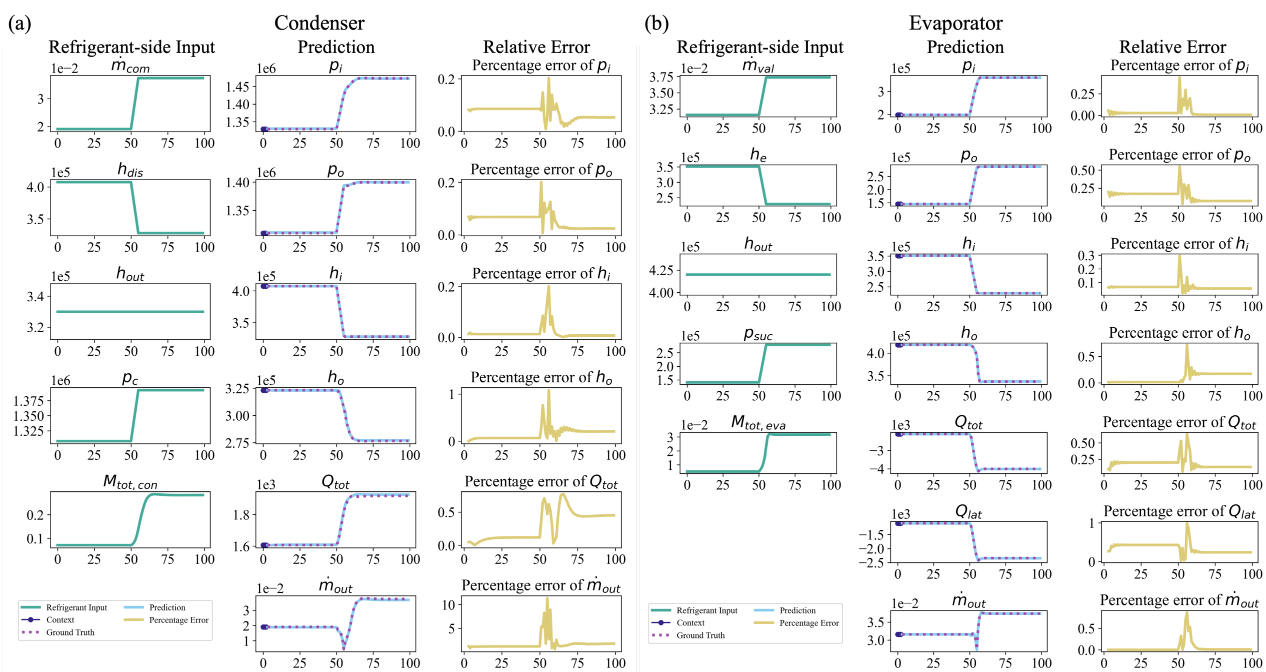


**Fig. 3** Multi-step inference and evaluation of the GRU models of HEXs for a time series in test set. (a) Condenser. (b) Evaporator.

**Table 1** Comparison between CNNGRU [12] and our GRU architecture on the average percentage error evaluated with the condenser and evaporator test sets.

| Component | Model | $p_1$ | $p_N$ | $h_1$ | $h_N$ | $Q_{tot}$ | $Q_{lat}$ | $\dot{m}_{out}$ |
|---|---|---|---|---|---|---|---|---|
| Condenser | CNN-GRU [12] | 0.09% | 0.38% | 0.03% | 0.33% | 2.04% | - | 15.10% |
| | Ours | **0.09%** | **0.06%** | 0.04% | 0.40% | **2.04%** | - | 16.10% |
| Evaporator | CNN-GRU [12] | 0.13% | 0.50% | 0.02% | 0.05% | 0.83% | 1.49% | 0.52% |
| | Ours | **0.06%** | **0.07%** | 0.07% | **0.05%** | **0.59%** | **0.81%** | **0.34%** |

A comparative analysis detailed in Table 1 highlights the performance of our GRU models relative to Chandrachur's CNN-GRU approach [12] for nonlinear HEX dynamics. Our GRU architecture not only matches but frequently beats CNN-GRU performance, especially in predicting evaporators and the pressures of condenser. The improvement in accuracy originates from our design choices, specifically the flexible context/prediction length and the usage of a student enforcing mechanism. Moreover, the inference on all the time series of the test set using our GRU architecture took only 2 minutes, greatly outbeating CNN-GRU's inference duration of 2 hr 33 minutes. It indicates that our GRU architecture possesses high capabilities for efficient individual HEX and system-level dynamic simulations compared to existing models.

However, predictions for the condenser $\dot{m}_{ref,out,con}$ during transient phases deviate from the ground truth, probably caused by the abrupt dynamic nature of condenser, resulting a wide and non-uniform range in $\dot{m}$ values and increasing the model training complexity. A potential solution involves designing a nonlinear normalization technique tailored for the feature $\Delta\dot{m}$, thereby modifying its distribution and improving prediction accuracy.

### 3.2 Hybrid Modeling For Vapor Compression System

*Experiment setup.* We then extended the boundaries of our research beyond individual components to study the full vapor compression cycle, through the adoption of a hybrid modeling framework developed in Section 2.4. The hybrid system model was set up with a simulation duration of 500s and a uniform time step of 1s, utilizing R134A as the working fluid. Our validation process involved two different system configurations, based on compressor speeds, to test the adaptability of the hybrid system model. Specifically:

- Normal-speed compressor system: compressor frequency $f = 55\text{Hz}$, valve coefficient $C_V = 0.01$
- High-speed compressor system: compressor frequency $f = 65\text{Hz}$, valve coefficient $C_V = 0.008$

Besides, both system configurations shared identical initial conditions as below:

$$\begin{aligned} &\text{(Compressor)} \quad V_{disp} = 1.14 * 10^{-5}\text{m}^3,\ \eta_V = 0.95,\ \eta_{isen} = 0.8 \\ &\text{(Condenser)} \quad p_{1,con} = 1.3 * 10^6\text{Pa}, p_{N,con} = 1.28 * 10^6\text{Pa}, h_{1,con} = 4.3 * 10^5\text{J/kg}, h_{N,con} = 2.7 * 10^5\text{J/kg} \\ &\text{(Evaporator)} \quad p_{1,con} = 4 * 10^5\text{Pa}, p_{N,con} = 3.98 * 10^5\text{Pa}, h_{1,con} = 2.9 * 10^5\text{J/kg}, h_{N,con} = 4.2 * 10^5\text{J/kg} \end{aligned} \tag{17}$$

During the simulation, the context lengths for the GRU models within the condenser and evaporator were initially set at $N$=2 and later increased to $N$=20 after $t$=20s, allowing broader historical data to be evaluated and thereby improving the transient state predictions. As the system stabilizes towards equilibrium, the context lengths were reverted to $N$=2, optimizing the simulation efficiency. For benchmarking, we generated physics-based simulation data using the Dymola 2020x compiler, mirroring the coefficient setup of the hybrid system model.

*Results and discussion.* The hybrid modeling simulation results for representative physical quantities are presented with benchmarking in Fig. 4 and Table 2. Fig. 4 represents the evolution of key physical parameters within two different system configurations, reflecting the dynamics of momentum, mass and energy throughout both transient and steady-state phases. Table 2 quantitatively provides a comparison of the hybrid and physics-based simulations, indicating high accuracy of the hybrid model, particularly in steady-state phases. Among two system configurations with different compressor speeds as shown in Fig. 4, most of the physical quantities in the hybrid model exhibited the similar trends as the physics-based model. Besides, the comparative analysis shown in Table 2 demonstrates that most physical quantities from the hybrid model simulation

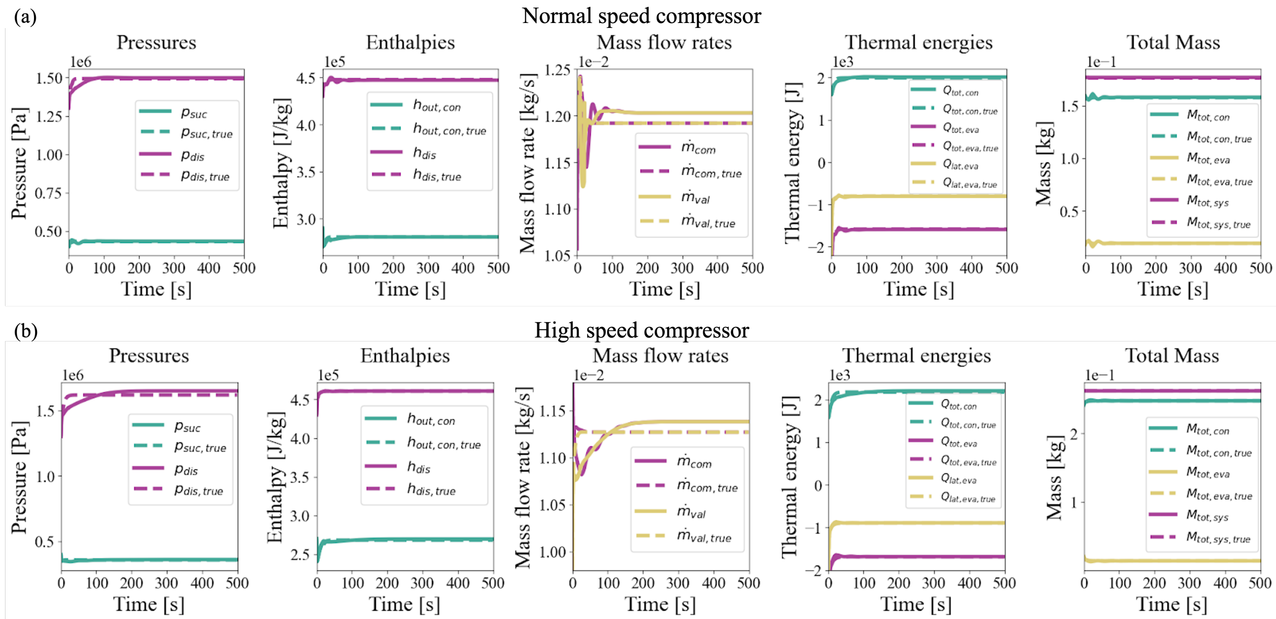


**Fig. 4** Hybrid modeling results of key physical quantities for the vapor compression cycle with (a) normal speed compressor (b) high speed compressor. Solid lines represent the hybrid modeling prediction values, while dashed lines represent the simulated ground truth form physics-based models.

**Table 2** Hybrid modeling results of key physical quantities in vapor compression cycle with normal and high speed compressor, respectively corresponding to Fig. 4(a,b). Rows from top to bottom stand for 'root mean-squared error of entire series', 'average percentage error of entire series', 'steady state percentage error'.

| Config. | Metrics | $m_{com}$ | $m_{val}$ | $p_{suc}$ | $p_{dis}$ | $h_{dis}$ | $h_{o,con}$ | $Q_{tot,con}$ | $Q_{tot,eva}$ | $Q_{lat,eva}$ | $M_{tot,con}$ | $M_{tot,eva}$ |
|---|---|---|---|---|---|---|---|---|---|---|---|---|
| Normal Speed Compressor | RMSE | 1.09E-04 | 1.17E-04 | 3.46E+03 | 1.43E+04 | 6.60E+02 | 7.25E+02 | 1.47E+01 | 1.15E+01 | 6.84E+00 | 8.17E-04 | 5.10E-04 |
| | Avg Error | **0.66%** | **0.60%** | **0.61%** | **0.4069%** | **0.11%** | **0.14%** | **0.32%** | **0.53%** | **0.62%** | **0.46%** | 1.52% |
| | SS Error | 0.45% | 0.45% | 0.48% | **0.11%** | **0.07%** | **0.06%** | **0.07%** | 0.35% | 0.42% | 0.43% | 0.83% |
| High Speed Compressor | RMSE | 1.74E-04 | 1.33E-04 | 3.60E+03 | 3.86E+04 | 2.88E+02 | 1.66E+03 | 5.24E+01 | 1.69E+01 | 1.18E+01 | 4.06E-04 | 2.70E-04 |
| | Avg Error | 1.11% | **0.99%** | **0.74%** | 1.96% | **0.04%** | **0.57%** | 1.62% | **0.57%** | 1.08% | **0.10%** | 1.12% |
| | SS Error | 0.87% | 0.92% | 0.61% | 1.99% | **0.02%** | 0.80% | 0.51% | 0.37% | 0.93% | **0.05%** | 0.79% |

entered the steady state with above 99% accuracy, including normal and high compressor speed scenarios. However, the model encounters certain challenges during transient phases, especially in the aspect of mass flow rate predictions. These results indicate the potential of the hybrid modeling framework in simulating accurate dynamics of the vapor compression system, but also highlight specific areas where further refinement is needed.

Another advantage of the hybrid model lies in the simulation speed, which reduces the simulation duration from 1 minute in the physics-based model down to 5s with our hybrid model, resulting from the efficiency of using GRU-based data-driven models within the hybrid framework. Moreover, the design of dynamically adjusting the context length during simulation — from a context length of $N$=2 to $N$=20 after 20s into the simulation and reverting to $N$=2 as the system approached steady state — allows a more comprehensive data context for the GRU model during transient states while not significantly sacrificing the simulation speed, improving the predictive accuracy and flexibility during these critical phases.

Besides, the conservation of mass is proven to be satisfied by the evidence of the constant total refrigerant mass $M_{tot,sys}$ and the equality of mass flow rates through various components at equilibrium. This is a direct outcome of the design of the hybrid modeling framework, which accounts for the conservation of mass not only in the development of root-finding solver, but also by the updates of total masses and change-in mass flow rates in the HEX components during each time step. These special design allows our proposed hybrid model to not only predict accurately at the system level but also adheres to fundamental physics principles.

Despite its strengths, our proposed hybrid model reveals certain limitations, with notable inaccuracies and lag in predicting the discharge pressure $p_{dis}$ during transient phases. This issue suggests a reassessment on the assumption of transferring potentially unchanged physical quantities between consecutive time steps, which can introduce and amplify errors into the GRU models. One solution is to revise the update mechanism, solving all physical quantities simultaneously rather than decomposing in two steps. This approach, though more computationally intensive, may improve accuracy. Alternatively, a smart optimization on the dynamic adjustment of the context length during the simulation might improve transient predictions. Further strategies could involve re-parameterizing the autoregressive models for HEX components or developing new data-driven models for other system elements.

## 4. CONCLUSIONS AND FUTURE WORK

In this study, we proposed a novel hybrid modeling framework, combining data-driven autoregressive models with physical constraints of conservation laws, to simulate vapor compression system dynamics. Compared to conventional physics-based models, our method significantly accelerates computation while preserving strong accuracy. However, improving transient state prediction remains an aspect for refinement.

Future efforts will focus on boosting the transient accuracy of our hybrid modeling framework. We also plan to extend the system configuration by including additional components, further enhancing our model ability in handling arbitrary configurations. Those improvements will push the boundaries of current simulation methodologies, inspiring the innovation in large-scale HVAC&R systems, revealing the potential of the hybrid modeling framework.

## ACKNOWLEDGMENTS

The authors wish to thank the support of Xiulong Liu from the department of Electrical and Computer Engineering at University of Washington.

## REFERENCES

[1] Qiao, H., Aute, V., and Radermacher, R., (2015) "Transient modeling of a flash tank vapor injection heat pump system – part i: Model development," *International Journal of Refrigeration*, 49, pp. 169–182.

[2] Belman-Flores, J., Ledesma, S., Garcia, M., Ruiz, J., and Rodríguez-Muñoz, J., (2013) "Analysis of a variable speed vapor compression system using artificial neural networks," *Expert Systems with Applications*, 40(11), pp. 4362–4369.

[3] Sanaye, S. and Asgari, H., (2013) "Thermal modeling of gas engine driven air to water heat pump systems in heating mode using genetic algorithm and artificial neural network methods," *International Journal of Refrigeration*, 36(8), pp. 2262–2277.

[4] Swider, D., Browne, M., Bansal, P., and Kecman, V., (2001) "Modelling of vapour-compression liquid chillers with neural networks," *Applied Thermal Engineering*, 21(3), pp. 311–329.

[5] Zhao, L., Cai, W.-J., and Man, Z.-H., (2014) "Neural modeling of vapor compression refrigeration cycle with extreme learning machine," *Neurocomputing*, 128, pp. 242–248.

[6] Li, Z.-Y., Shao, L.-L., and Zhang, C.-L., (2015) "Fin-and-tube condenser performance modeling with neural network and response surface methodology," *International Journal of Refrigeration*, 59, pp. 124–134.

[7] Li, Z.-Y., Shao, L.-L., and Zhang, C.-L., (2016) "Modeling of Finned-Tube Evaporator Using Neural Network and Response Surface Methodology," *Journal of Heat Transfer*, 138(5), pp. 051502.

[8] Ledesma, S., Belman-Flores, J., and Barroso-Maldonado, J., (2015) "Analysis and modeling of a variable speed reciprocating compressor using ann," *International Journal of Refrigeration*, 59, pp. 190–197.

[9] Wan, H., Cao, T., Hwang, Y., and Oh, S., (2019) "An electronic expansion valve modeling framework development using artificial neural network: A case study on vrf systems," *International Journal of Refrigeration*, 107, pp. 114–127.

[10] Qiao, H., Laughman, C. R., Burns, D. J., and Bortoff, S. A., (2017) "Dynamic characteristics of an r-410 a multi-split variable refrigerant flow air-conditioning system," *12th IEA Heat Pump Conference*, 3(1), pp. 4.

[11] Cho, K., van Merriënboer, B., Gulcehre, C., Bahdanau, D., Bougares, F., Schwenk, H., and Bengio, Y., (2014) "Learning phrase representations using RNN encoder–decoder for statistical machine translation," *Proceedings of the 2014 Conference on Empirical Methods in Natural Language Processing (EMNLP)*, pp. 1724–1734.

[12] Bhattacharya, C., Chakrabarty, A., Laughman, C., and Qiao, H., (2022) "Modeling nonlinear heat exchanger dynamics with convolutional recurrent networks," *2nd Modeling, Estimation and Control Conference MECC*, 55(37), pp. 99–106.